



Magnetic resonance imaging evaluation of Yukatan minipig brains for neurotherapy applications

Seung Pil Yun¹, Dong Hyun Kim², Jung Min Ryu¹, Jae Hong Park¹, Su Shin Park¹, Ji Hoon Jeon¹,
Bit Na Seo¹, Hyun-Jeong Kim³, Jun-Gyu Park³, Kyoung-Oh Cho³, Ho Jae Han^{4*}

¹Department of Veterinary Physiology, College of Veterinary Medicine, Chonnam National University, Gwangju, Korea

²Department of Diagnostic Radiology, College of Medicine, Chosun University Hospital, Gwangju, Korea

³College of Veterinary Medicine, Biotherapy Human Resources Center, Chonnam National University, Gwangju, Korea

⁴Department of Veterinary Physiology, College of Veterinary Medicine and Research Institute for Veterinary Science, Seoul National University, Seoul, Korea

Magnetic resonance imaging (MRI) of six Yukatan minipig brains was performed. The animals were placed in stereotaxic conditions currently used in experiments. To allow for correct positioning of the animal in the MRI instrument, landmarks were previously traced on the snout of the pig. To avoid movements, animal were anesthetized. The animals were placed in a prone position in a Siemens Magnetom Avanto 1.5 System with a head coil. Axial T2-weighted and sagittal T1-weighted MRI images were obtained from each pig. Afterwards, the brains of the pigs were fixed and cut into axial sections. Histologic and MR images were compared. The usefulness of this technique is discussed.

Key words: Brain, Yukatan minipigs, magnetic resonance imaging, neurologic disorder

Received 7 November 2011; Revised version received 1 December 2011; Accepted 10 December 2011

Animal models of human diseases have always played a central role in biomedical research for the exploration and development of new therapies [1,2]. However, the evolutionary gap between humans and many of the applied animal models has hampered the direct application of knowledge gained from these studies to human therapy. In this regard, pigs share a number of anatomical and physiological characteristics with humans, which potentially make them a better model for some procedures and studies compared to other large animal species [1,3,4]. Minipigs are a major animal species used in translational research and are increasingly being used as an alternative to dogs and monkeys in biomedical research [5]. There is a large body of literature available detailing the normal anatomy and physiology of the species [5]. When different breeds are age-matched, organ sizes reflect the increased size of domestic breeds compared to miniature breeds; however, the physiologic functions are similar [6]. Conversely, when animals are weight-matched,

the sizes are similar for organs and structures; however, the physiologic functions are related to the relative maturity of the animals [6]. There are various swine strains available, each with its own characteristics including size and weight, which of course can influence data [6]. The most common miniature breeds available in the United States are the Hanford, Yukatan (mini), Sinclair and Göttingen (from largest to smallest) [7-10]. However, to our knowledge, there are no data on the macroscopic or microscopic background descriptions of Yukatan minipigs in the laboratory setting.

The pig brain is relatively large, with structures typical of other mammals [11,12]. The pig central nervous system (CNS) and the brain in particular have rapidly evolved as a model system for humans given both its size and anatomic characteristics [12]. Pigs have a gyrencephalic brain which predominantly consists of white matter with similar developmental peaks to that of humans [13,14]. Accurate determination of neuronal coordinates is necessary for precise

*Corresponding author: Ho Jae Han, Department of Veterinary Physiology, College of Veterinary Medicine, Seoul National University, 1 Daehakro, Gwanak-gu, Seoul 151-741, Korea
Tel: +82-2-880-1261; Fax: +82-2-887-2732; E-mail: hjhan@snu.ac.kr

This is an Open Access article distributed under the terms of the Creative Commons Attribution Non-Commercial License (<http://creativecommons.org/licenses/by-nc/3.0>) which permits unrestricted non-commercial use, distribution, and reproduction in any medium, provided the original work is properly cited.

and reliable biomedical research. These specifications can be verified with the use of magnetic resonance imaging (MRI) which allows for repeated examination of brain anatomy in live animals [15]. Recent developments in MRI hardware (radiofrequency coils, magnet design and receiver systems), together with improved pulse sequences, have facilitated acquisition with sub-millimeter resolution [16]. Accordingly, MRI-based stereotaxic procedures are currently of significant interest in neural research, including deep brain stimulation and cell transplantation [16-18]. Calculation of coordinates in the minipig has previously been restricted by insufficient structural information from MRI, excluding direct targeting. Furthermore, no intracranial stereotaxic reference points, standard-space null points or standard target coordinates have yet been established in this species. Therefore, this study was conducted to determine optimal conditions necessary for the use of MRI in Yukatan minipig stereotaxic procedures and to examine anatomic characteristics specific to Yukatan minipigs.

Materials and Methods

Animal handling

All experimental protocols were approved by the Ethics Committee of Chonnam National University (CNU IACUCYB-2008-29). The study was conducted on six physically healthy female Yukatan minipigs purchased from PWG Genetics Korea (Pyeongtaek, Korea). Animals were housed in individual cages at the central animal facility and received standard pig meal *ad libitum*. Prior to MRI procedures, all animals were fasted for a minimum of 24 h. Pigs were premedicated with an intramuscular injection of Azaperone® (0.5 mg/kg; SF Inc, Ansan, Korea) and xylazine (Rompun®, 8 mg/kg; Bayer Korea, Seoul, Korea), and anesthetized with an intramuscular injection of a combination of zolazepam/tiletamine (Zoletil®, 4.4 mg/kg; Virbac, Carros, France).

Hematoxylin and eosin (H&E) staining

For euthanasia, pigs were anesthetized with an intravenous injection of sodium pentobarbital (Entobal®, 100 mg/kg; Hanlim Pharm, Seoul, Korea), and executed by electrocution. After euthanasia, formalin-fixed and paraffin-embedded sections from brain tissue were stained with Mayer's H&E and examined microscopically.

MRI protocol

The animals were placed in a prone position in a Siemens Magnetom Avanto 1.5 System (Siemens Healthcare, Erlangen, Germany) with a head coil. Axial T2-weighted and sagittal

Table 1. MRI protocol parameters

	T2-weighted images	T1-weighted images
Direction	Axial (3 directions)	Sagittal
Protocol	Turbo spine echo	Spin echo
Slice thickness	3 mm	4 mm
TR	4,300 msec	364 msec
TE	96 msec	10 msec
Nex (averages)	7	2
Bandwidth	191 kHz	191 kHz
Base resolution	512	384
Phase resolution	60%	70%
Flip angle	150 degree	90 degree
Dist. Factor	10%	10%
FOV read	150 mm	230 mm
FOV phase	79.7%	100%

T1-weighted MRI images were obtained from each pig; axial view directions differed (Figure 2). The sequence was optimized to improve spatial resolution, the signal-to-noise-ratio and contrast. Furthermore, the sequence was performed within a reasonable acquisition time acceptable for *in vivo* imaging and survival studies. MRI parameters are shown in Table 1. The acquired images were adjusted for brightness and contrast to aid in the identification of structures.

Results

To perform MRI in Yukatan minipigs, we took advantage of the unique organization of the Yukatan minipig brains, whose anatomy includes the cortex and the gyrus (Figure 1A) [12]. The superior, lateral and inferior views of a perfusion-fixed whole brain are shown in Figures 1B-1D. In addition, it should be noted that MRI visualizes organs with a slight geometric distortion. This is often insignificant in clinical procedures, but can be an important factor in stereotaxic procedures. To confirm stereotaxic procedures and existence of artifacts, we have done a comparative analysis with various histological sections and MR images (Figures 1E-1H). As shown in Figure 1G, the phase-encoding axis is prone to scanner-induced artifacts and phase-dependent flow artifacts were also found on all our images at the level of the large vessels of the neck. In contrast, the round contour of the column of fornix and the mammillo-thalamic tract on coronal histological sections were also round and undistorted on the acquired images with no blurring of the edges or duplication of the structures. Therefore, image artifacts in the phase-encoding direction were considered minor using the protocol proposed in our study. The anatomical landmarks similar to other mammals were identified by MRI in the Yukatan minipig brain.

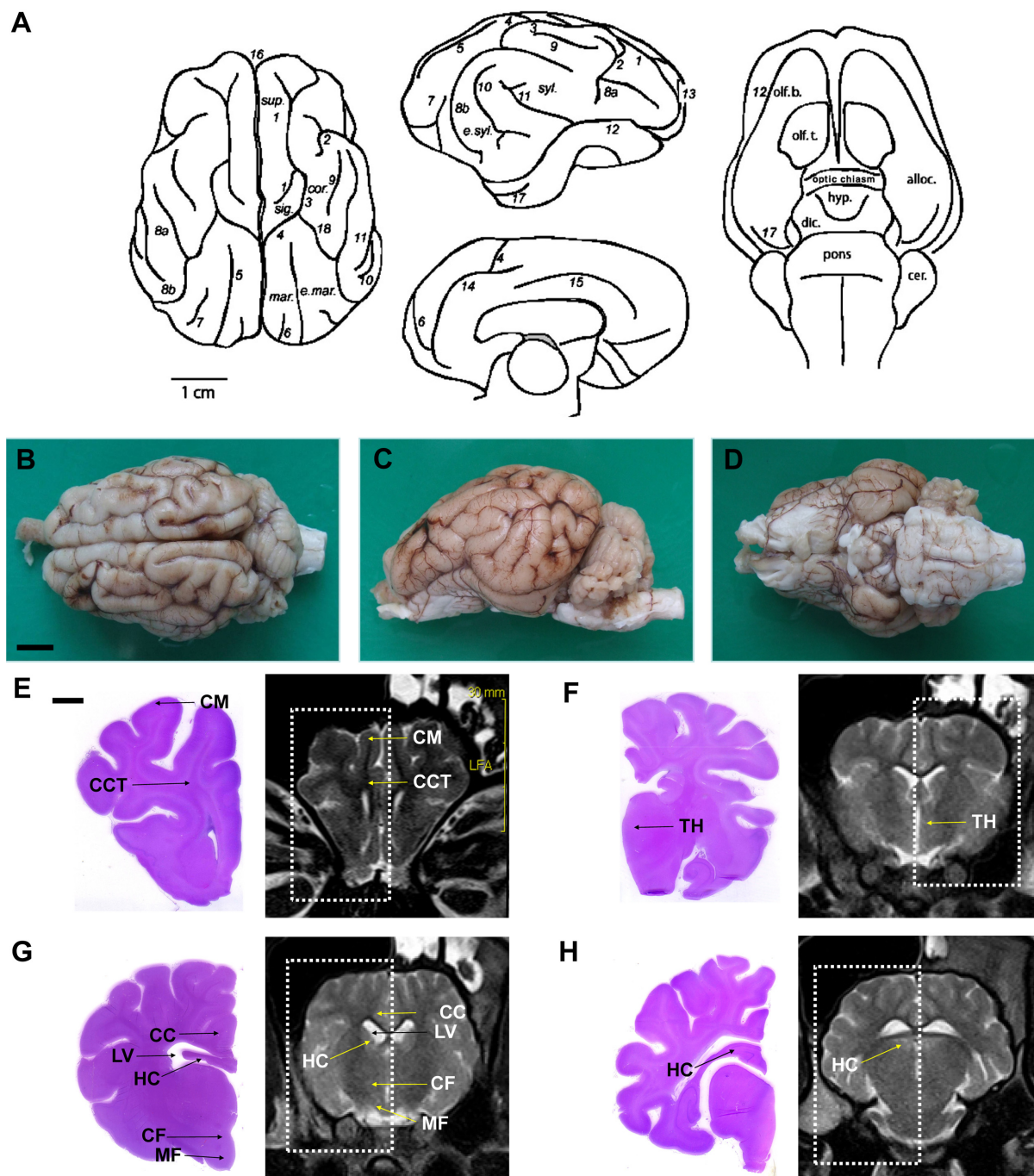


Figure 1. A minipig brain depicting (A) drawings of sulci and gyri patterns: (1) cruciate sulcus; (2) diagonal sulcus; (3) coronal sulcus; (4) ansate sulcus; (5) lateral sulcus; (6) entolateral sulcus; (7) ectolateral sulcus; (8) suprasylvii sulcus, (a) anterior, (b) posterior; (9) sulcus naris; (10) ectosylvia sulcus; (11) sylvii sulcus; (12) rhinal sulcus; (13) praesylvii sulcus; (14) splenial sulcus; (15) cingulate sulcus; (16) longitudinal sulcus; (17) sagittal sulcus; (18) coronal sulcus. cer., cerebellum; cor., coronal gyrus; dic., diencephalons; e.mar., ectomarginal gyrus; e.syl., ectosylvian gyrus; hyp., hypothalamus; mar., marginal gyrus; olf. b., olfactory bulb; olf. t., olfactory tubercle; sig., sigmoid gyrus; sup., superior frontal gyrus; syl., sylvian gyrus [23]. Scale bars represent 1 cm. (B) superior, (C) lateral and (D) inferior view of a perfusion-fixed whole brain. Normal structures of cerebrum, axial section. Scale bars represent 1 cm. H&E-stained histological section and MR image at the level of the anterior of corpus callosum (E) and the optic chiasm region (F). (G) Histological section and MR image at the level of the mammillo-thalamic tract (MF) and the column of fornix (CF) seen as four hypothalamic, delicately stained rounded structures. In the corresponding MRI, CF dorsally and MF ventrally are found as four round structures in the hypothalamus. (H) Histological section and MR image at the level of the front of posterior of corpus callosum. Scale bars represent 0.5 cm. CM, cerebral medulla; CCT, cerebral cortex; TH, thalamus; LV, lateral ventricle; CC, corpus callosum; HC, hippocampus.

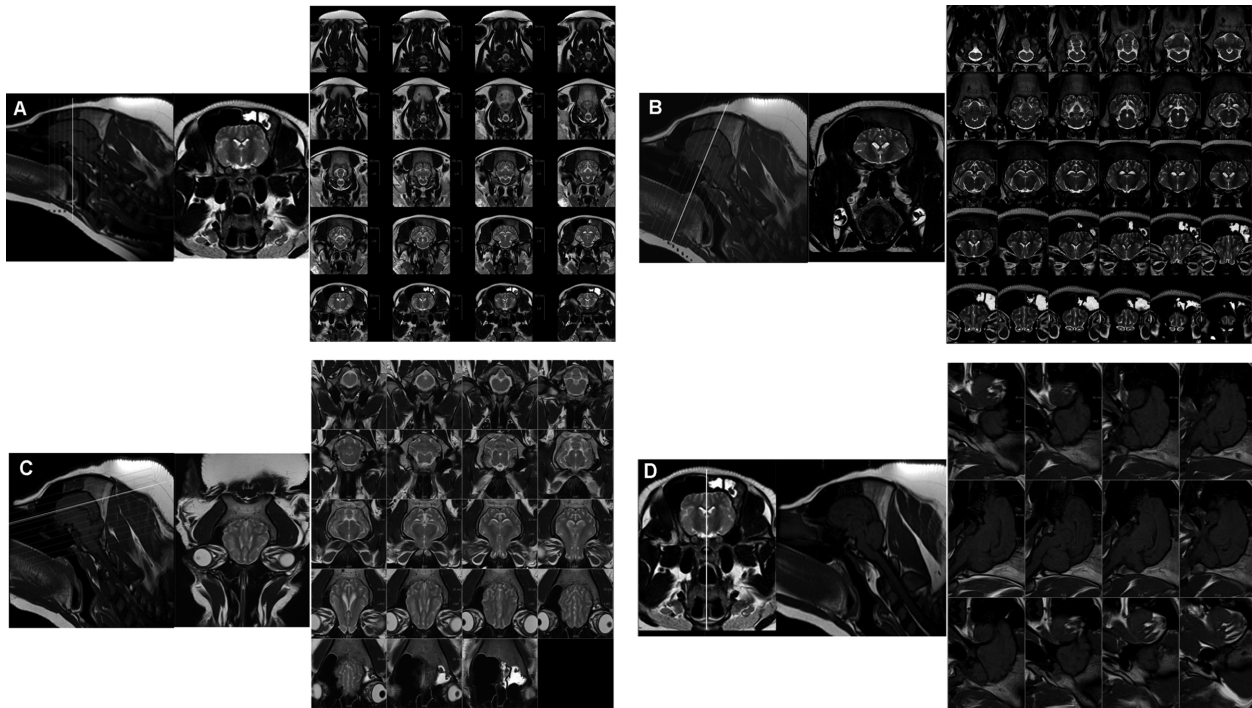


Figure 2. A topogram showing the three different axial directions of scanning on T2- (A-C) and sagittal T1-weighted images (D). white line is the reference line.

T2- and T1-weighted imaging sequences provided good contrast and spatial resolution for identification of most clinically relevant brain anatomy in both the axial and sagittal planes (Figure 2). However, T2-weighted images were the most useful for identifying clinically relevant neuroanatomy. Using a slice thickness of 3.0 mm enabled reduced-volume averaging and improved spatial resolution of smaller structures (Figures 3-4). Axial plane images are shown in Figure 3. Sagittal plane images are shown in Figure 4. The striatum was fairly large, appearing as two compartments, namely the putamen and caudate nucleus. The caudate nucleus is an elongated mass of gray matter which is closely related to the lateral ventricle. The putamen is the largest part of the striatum and its most rostral portion is located lateral to the head of the caudate nucleus, separated by the anterior part of the internal capsule. The putamen is separated from cortical tissue by the external capsule (Figure 3). On sagittal T1-weighted MR images of the posterior pituitary lobe, the adenohypophysis is isointense relative to gray matter and the neurohypophysis is hyperintense (Figure 4). The globus pallidus forms the more medial part of the stratum and it is separated from the putamen by a thin layer of white matter called the lateral medullary lamina (Figures 5A-5C). The substantia nigra was identified as a broad band of gray matter dorsal to the cerebral peduncle extending from the level of the red nucleus (Figure 6A). The entire hippocampus could be

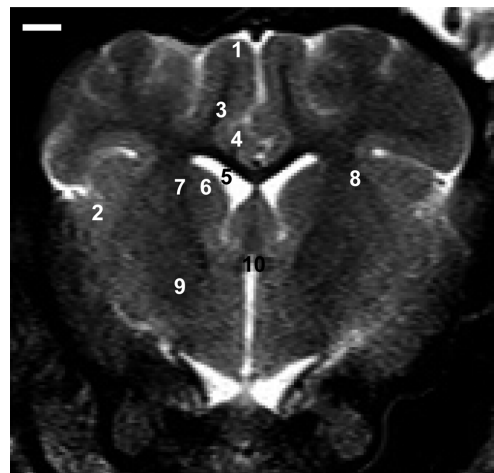


Figure 3. Representative axial T2-weighted images at the anterior commissure level. Frontal cortex (1), temporoparietal cortex (2), subcortical white matter (3), corpus callosum (4), lateral ventricle (5), caudate nucleus (6), internal capsule (7), putamen (8), globus pallidus (9), and anterior commissure (10) are present. Scale bar represents 0.5 cm.

visualized (Figures 6A-6C). Also, on sagittal T1-weighted MR images of the hippocampus could be visualized (Figure 6D).

Discussion

Animal models of human diseases have played a central role in biomedical research for the exploration and development

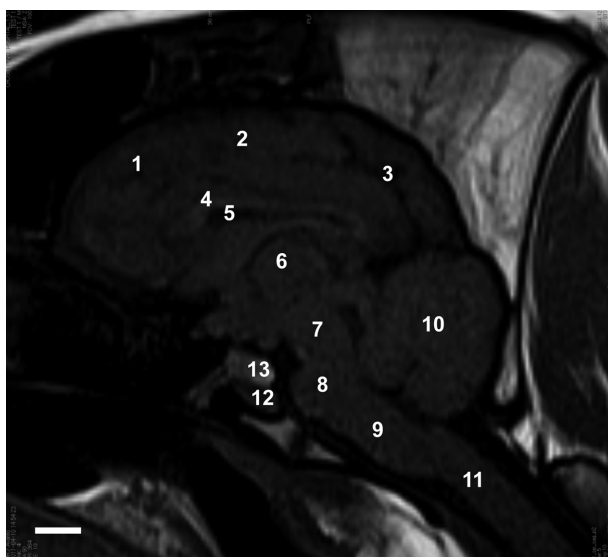


Figure 4. Sagittal T1-weighted MRI. frontal lobe (1), parietal lobe (2), occipital lobe (3), corpus callosum (4), lateral ventricle (5), thalamus (6), midbrain (7), pons (8), medulla oblongata (9), cerebellum (10), spinal cord (11), adenohypophysis (12), and neurohypophysis (13). Sagittal T1-weighted MRI shows the posterior pituitary lobe. The adenohypophysis is isointense relative to gray matter and the neurohypophysis is hyperintense. Scale bar represents 1 cm.

of new therapies [19,20]. However, the evolutionary gap between humans and many of the applied animal models has continued to hamper direct applicability of the knowledge gained for human therapy [20,21]. Although the non-human primate model appears ideal, technical and organizational difficulties and high costs dictate the need for an alternative species. Therefore, we require animal models that reflect the geometry and complexity of the cytoarchitecture found in the human CNS as closely as possible, that are more affordable

than primates. Minipigs have a relatively large brain with a human-like blood supply and immunologic response characteristics [16,20]. However, the topology of the pig hippocampus, hidden within the temporal lobe, indicates a degree of encephalization, an anatomical difference falling somewhere between that of the rodent and human brain [22]. In general, the organization of the main cortical lobes in the pig brain differs somewhat from that of humans and lacks the pronounced caudal expansion and curvature of the progressive telencephalon observed in primates [12]. Although these differences exist between pig and human brains, the pig brain, which is gyrencephalic, resembles the human brain more in anatomy, growth and development than the brains of commonly used small laboratory animals [12]. Furthermore, similarities in the gross anatomy of the pig brain to that of humans has also been demonstrated for the hippocampus, a limbic structure [23,24], as well as for subcortical and diencephalic nuclei [25,26] and brainstem structures [27,28]. Thus, the size of the pig brain permits the identification of cortical and subcortical structures by imaging techniques [12]. The CNS size and physiology and the longer lifespan of swine make them suitable for long-term evaluation of the safety and efficacy of cell therapies for CNS disorders [29,30].

While non-invasive methods for identifying the function of a particular brain region are now well established, there is still a challenge to relate location to architecture identified microscopically [31]. Here, we describe how imaging technology can now be used to identify anatomical regions based on the underlying myeloarchitecture in the living Yukatan minipig brain. Neurologic and neurodegenerative disorders and typical lesion locations as described in Table

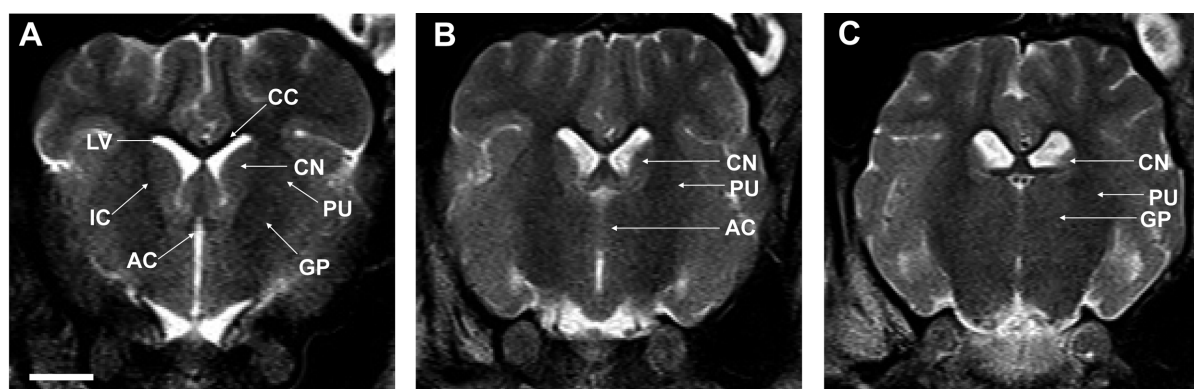


Figure 5. Striatum identified as a large two-compartment structure divided into the putamen (PU) and the caudate nucleus (CN) by the internal capsule (IC). Laterally, the PU is separated from the cortical tissue by the external capsule (A). Posteriorly, only the tail of the CN is visualized and the PU becomes dominate. The anterior commissure (AC) connects the hemispheres ventrally (B). At the AC level, a band of white substance, pars posterior of the AC, separates the most posterior parts of the PU from the globus pallidus (GP). Subdivision of the GP into internal and external segments was not possible (C). Scale bar represents 1 cm. LV, lateral ventricle; CC, corpus callosum.

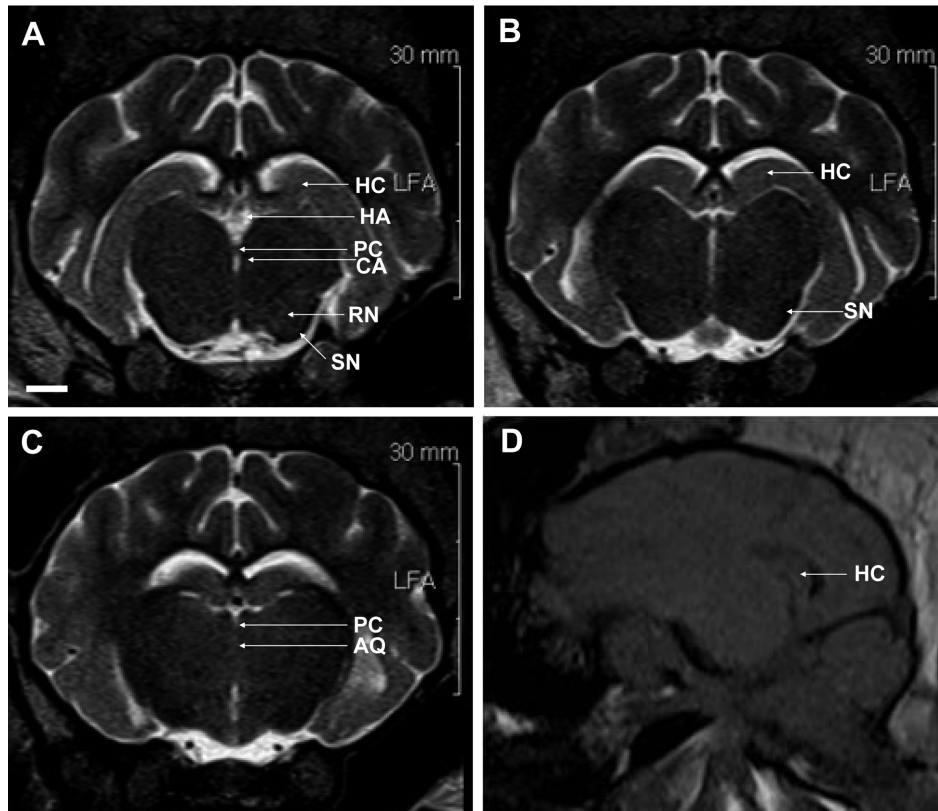


Figure 6. The substantia nigra (SN) is seen as a band of white matter dorsal to the dark cerebral peduncle, ventro-lateral to the bilaterally visible red nucleus (RN), a distinct rounded structure separated from the midline by the midbrain tegmentum. Habenular nuclei (HA) are also visualized. The hippocampus is seen in its full extent dorsal to the thalamus, sweeping around it to the temporal lobe (A-C). Sagittal T1-weighted MRI shows the hippocampus (D). Scale bar represents 0.5 cm. HC, hippocampus; HA, habenular nuclei; PC, posterior commissure; CA, cerebral aqueduct; SN, substantia nigra; RN, red nucleus; AQ, cerebral aqueduct.

Table 2. Disease-related anatomic targets

Disease	Typical lesion location
Amyotrophic lateral sclerosis (ALS; Lou Gehrig's disease)	Upper and lower motor neurons (frontal cortex and spinal cord)
Parkinson's disease (PD)	Nigrostriatal dopaminergic neurons
Alzheimer's disease (AD; dementia)	Hippocampus (early phase), entorhinal cortex, frontal, temporal and parietal association cortex
Frontotemporal lobar degeneration (FTLD)	Frontal and anterior temporal cortex (early phase), hippocampus
Dementia with Lewy bodies	Nigrostriatal dopaminergic neuron, frontal cortex, hippocampus, forebrain cholinergic neurons
Stroke	Hippocampus, frontoparietal cortex, striatum
Epilepsy	Temporal cortex, entorhinal cortex, hippocampus
Depression	Ventral tegmental area, amygdala, nucleus accumbens, septum, prefrontal cortex
Cluster headache	Hypothalamus (posterior part)
Dystonia	Globus pallidum
Tourette's syndrome	The centromedian thalamic nucleus, internal capsule, globus pallidum
Obsessive-compulsive disorder	Internal capsule, ventral striatum, accumbens nucleus

2 are adapted from a syndrome approach to clinical neurology [32,33]. This approach attributes predictable neurodegenerative or neurologic signs to disruption of specific tracts, nuclei or nerves within one or more of the embryologic subdivisions of the brain [15,16]. As shown in Table 2, multifocal lesions or diffuse brain disease will

also usually present with multiple neurologic signs, making neuroanatomic localization more complex.

Most people are familiar with MRI scans of the brain and the way they depict the internal structures of this fascinating organ [31]. The most striking feature in such scans, apart from the overall shape of the pig head, is the distinction

between the convoluted surface of the brain, the cerebral cortex and the white matter connections that join different parts of the brain [31]. While MRI is useful to map the concentration of water in structures being imaged, the distinction between white matter and grey matter is resolved in a much more subtle way [16]. In the future, high-resolution MRI could become a standard method of detecting pathological changes in the brain at the earliest possible occasion, leading to early treatment and minimization of irreversible damage. In the present study, we used T1/2-weighted MRI results from six Yukatan minipigs as the basis for developing a volumetric and stereotaxic pig brain atlas. Automatic coregistration of the pig brain was obtained using 12 degrees of freedom, rather than 9 degrees typically used in human studies [34]. The relatively greater spatial uniformity of the smaller pig brain facilitates coregistration with a higher number of fitting parameters [34]; thus, the 3D surface rendering of the average pig brain preserves the major sulcal anatomy. In particular, the Sylvian fissure and the coronal fissure can clearly be seen in the average brain surface rendering. However, the fine details of sulcal and gyral anatomy were lost in the coregistration and averaging process. Furthermore, the detailed segmentation of subcortical structures is impossible to see with the present 1-T imaging. New MR data to be acquired with a 3-T magnet and with longer scanning times should improve the surface rendering of the pig brain and also reveal subcortical anatomic details. Current efforts are directed toward the registration of high-field images to histologic material sectioned in the anatomical planes defined in the common coordinate system. Although various researches on swine brain strains by MR imaging was reported, minipig brain research is concentrated in the most common or smallest miniature breeds such as Göttingen [16]. Our study provided moderate miniature breed data on macroscopic or microscopic background descriptions in the laboratory setting. Also, this work provides the basis for a planned systemic comparison of gender, age and strain differences in minipig neuroanatomy for the bio-organ research field.

Acknowledgments

This work was supported by a grant (code# 20070401034006) from the BioGreen 21 Program, Rural Development Administration, Korea. The authors acknowledge a graduate fellowship provided by the Ministry of Education and Human Resources Development through the Brain Korea 21 project of Korea.

References

1. Dooldeniya MD, Warrens AN. Xenotransplantation: Where are we today? *J R Soc Med* 2003; 96(3): 111-117.
2. Lee KT, Byun MJ, Kang KS, Park EW, Lee SH, Cho S, Kim H, Kim KW, Lee T, Park JE, Park W, Shin D, Park HS, Jeon JT, Choi BH, Jang GW, Choi SH, Kim DW, Lim D, Park MR, Ott J, Schook LB, Kim TH. Neuronal genes for subcutaneous fat thickness in human and pig are identified by local genomic sequencing and combined SNP association study. *PLoS One* 2011; 6(2): e16356.
3. Hammer C. Xenotransplantation - will it bring the solution to organ shortage? *Ann Transplant* 2004; 9(1): 7-10.
4. Hannon JP, Bossone CA, Wade CE. Normal physiological values for conscious pigs used in biomedical research. *Lab Anim Sci* 1990; 40(3): 293-298.
5. Thors A, Muck P. Resorbable inferior vena cava filters: trial in an *in-vivo* porcine model. *J Vasc Interv Radiol* 2011; 22(3): 330-335.
6. Lomber G. Animal models. *Pancreatol* 2006; 6(5): 427-428.
7. Ahn YK, Ryu JM, Jeong HC, Kim YH, Jeong MH, Lee MY, Lee SH, Park JH, Yun SP, Han HJ. Comparison of cardiac function and coronary angiography between conventional pigs and micropigs as measured by multidetector row computed tomography. *J Vet Sci* 2008; 9(2): 121-126.
8. Andersen F, Watanabe H, Bjarkam C, Danielsen EH, Cumming P. Pig brain stereotaxic standard space: mapping of cerebral blood flow normative values and effect of MPTP-lesioning. *Brain Res Bull* 2005; 66(1): 17-29.
9. Ho CS, Martens GW, Amoss MS, Jr., Gomez-Raya L, Beattie CW, Smith DM. Swine leukocyte antigen (SLA) diversity in Sinclair and Hanford swine. *Dev Comp Immunol* 2010; 34: 250-257.
10. Mezrich JD, Haller GW, Arn JS, Houser SL, Madsen JC, Sachs DH. Histocompatible miniature swine: an inbred large-animal model. *Transplantation* 2003; 75(6): 904-907.
11. Jelsing J, Gundersen HJ, Nielsen R, Hemmingsen R, Pakkenberg B. The postnatal development of cerebellar Purkinje cells in the Göttingen minipig estimated with a new stereological sampling technique--the vertical bar fractionator. *J Anat* 2006; 209(3): 321-331.
12. Lind NM, Moustgaard A, Jelsing J, Vajta G, Cumming P, Hansen AK. The use of pigs in neuroscience: modeling brain disorders. *Neurosci Biobehav Rev* 2007; 31(5): 728-751.
13. Dullemeijer C, Zock PL, Coronel R, Den Ruijter HM, Katan MB, Brummer RJ, Kok FJ, Beekman J, Brouwer IA. Differences in fatty acid composition between cerebral brain lobes in juvenile pigs after fish oil feeding. *Br J Nutr* 2008; 100(4): 794-800.
14. Smith DH, Cecil KM, Meaney DF, Chen XH, McIntosh TK, Gennarelli TA, Lenkinski RE. Magnetic resonance spectroscopy of diffuse brain trauma in the pig. *J Neurotrauma* 1998; 15(9): 665-674.
15. Marcilloux JC, Félix MB, Rampin O, Stoffels C, Ibazizen MT, Cabanis EA, Laplace JP, Albe-Fessard D. Preliminary results of a magnetic resonance imaging (MRI) study of the pig brain placed in stereotaxic conditions. *Neurosci Lett* 1993; 156(1-2): 113-116.
16. Rosendal F, Pedersen M, Sangill R, Stodkilde-Jørgensen H, Nielsen MS, Bjarkam CR, Sunde N, Sørensen JC. MRI protocol for *in vivo* visualization of the Göttingen minipig brain improves targeting in experimental functional neurosurgery. *Brain Res Bull* 2009; 79(1): 41-45.
17. Danielsen EH, Cumming P, Andersen F, Bender D, Brevig T, Falborg L, Gee A, Gillings NM, Hansen SB, Hermansen F, Johansen J, Johansen TE, Dahl-Jørgensen A, Jørgensen HA,

- Meyer M, Munk O, Pedersen EB, Poulsen PH, Rodell AB, Sakoh M, Simonsen CZ, Smith DF, Sorensen JC, Ostergard L, Zimmer J, Gjedde A, Moller A. The DaNeX study of embryonic mesencephalic, dopaminergic tissue grafted to a minipig model of Parkinson's disease: preliminary findings of effect of MPTP poisoning on striatal dopaminergic markers. *Cell Transplant* 2000; 9(2): 247-259.
18. Jelsing J, Olsen AK, Cumming P, Gjedde A, Hansen AK, Arnfred S, Hemmingsen R, Pakkenberg B. A volumetric screening procedure for the Göttingen minipig brain. *Exp Brain Res* 2005; 162(4): 428-435.
 19. Ruehe B, Niehues S, Heberer S, Nelson K. Miniature pigs as an animal model for implant research: bone regeneration in critical-size defects. *Oral Surg Oral Med Oral Pathol Oral Radiol Endod* 2009; 108(5): 699-706.
 20. Vodicka P, Smetana K Jr, Dvorankova B, Emerick T, Xu YZ, Ourednik J, Ourednik V, Motlik J. The miniature pig as an animal model in biomedical research. *Ann N Y Acad Sci* 2005; 1049: 161-171.
 21. Hassold T, Hunt P. To err (meiotically) is human: the genesis of human aneuploidy. *Nat Rev Genet* 2001; 2(4): 280-291.
 22. Holm IE, West MJ. Hippocampus of the domestic pig: a stereological study of subdivisional volumes and neuron numbers. *Hippocampus* 1994; 4(1): 115-125.
 23. Dilberovic F, Secerov D, Tomic V. Morphological characteristics of the gyrus dentatus in some animal species and in man. *Anat Anz* 1986; 161(3): 231-238.
 24. Holm IE, Geneser FA. Histochemical demonstration of zinc in the hippocampal region of the domestic pig: I. Entorhinal area, parasubiculum, and presubiculum. *J Comp Neurol* 1989; 287(2): 145-163.
 25. Felix B, Leger ME, Albe-Fessard D, Marcilloux JC, Rampin O, Laplace JP. Stereotaxic atlas of the pig brain. *Brain Res Bull* 1999; 49(1-2): 1-137.
 26. Larsen MO, Rolin B. Use of the Göttingen minipig as a model of diabetes, with special focus on type 1 diabetes research. *ILAR J* 2004; 45(3): 303-313.
 27. Freund E. Cytoarchitectonics of the mesencephalon and pons in the domestic pig (*Sus scrofa domestica*). *Anat Anz* 1969; 125(4): 345-362.
 28. Ostergaard K, Holm IE, Zimmer J. Tyrosine hydroxylase and acetylcholinesterase in the domestic pig mesencephalon: an immunocytochemical and histochemical study. *J Comp Neurol* 1992; 322(2): 149-166.
 29. Dall AM, Danielsen EH, Sorensen JC, Andersen F, Moller A, Zimmer J, Gjedde AH, Cumming P. Quantitative [¹⁸F]fluorodopa/PET and histology of fetal mesencephalic dopaminergic grafts to the striatum of MPTP-poisoned minipigs. *Cell Transplant* 2002; 11(8): 733-746.
 30. Smith PM, Blakemore WF. Porcine neural progenitors require commitment to the oligodendrocyte lineage prior to transplantation in order to achieve significant remyelination of demyelinated lesions in the adult CNS. *Eur J Neurosci* 2000; 12(7): 2414-2424.
 31. Bridge H, Clare S. High-resolution MRI: *in vivo* histology? *Philos Trans R Soc Lond B Biol Sci* 2006; 361(1465): 137-146.
 32. Benabid AL. What the future holds for deep brain stimulation. *Expert Rev Med Devices* 2007; 4(6): 895-903.
 33. Pereira EA, Green AL, Nandi D, Aziz TZ. Deep brain stimulation: indications and evidence. *Expert Rev Med Devices* 2007; 4(5): 591-603.
 34. Black KJ, Snyder AZ, Koller JM, Gado MH, Perlmutter JS. Template images for nonhuman primate neuroimaging: 1. Baboon. *Neuroimage* 2001; 14(3): 736-743.